Applied and Environmental Microbiology, Nov. 2007, p. 6842–6853 Vol. 73, No. 21
0099-2240/07/$08.00+0 doi:10.1128/AEM.00597-07

Impact of Substrate Glycoside Linkage and Elemental Sulfur on Bioenergetics of and Hydrogen Production by the Hyperthermophilic Archaeon *Pyrococcus furiosus*▽†

Chung-Jung Chou,[1] Keith R. Shockley,[1]‡ Shannon B. Conners,[1]§ Derrick L. Lewis,[1] Donald A. Comfort,[1]¶ Michael W. W. Adams,[2] and Robert M. Kelly[1]*

Department of Chemical and Biomolecular Engineering, North Carolina State University, Raleigh, North Carolina 27695-7905,[1] *and Department of Biochemistry and Molecular Biology, University of Georgia, Athens, Georgia 30602-7229*[2]

Received 15 March 2007/Accepted 26 August 2007

Glycoside linkage (cellobiose versus maltose) dramatically influenced bioenergetics to different extents and by different mechanisms in the hyperthermophilic archaeon *Pyrococcus furiosus* when it was grown in continuous culture at a dilution rate of 0.45 h^{-1} at 90°C. In the absence of S^0, cellobiose-grown cells generated twice as much protein and had 50%-higher specific H_2 generation rates than maltose-grown cultures. Addition of S^0 to maltose-grown cultures boosted cell protein production fourfold and shifted gas production completely from H_2 to H_2S. In contrast, the presence of S^0 in cellobiose-grown cells caused only a 1.3-fold increase in protein production and an incomplete shift from H_2 to H_2S production, with 2.5 times more H_2 than H_2S formed. Transcriptional response analysis revealed that many genes and operons known to be involved in α- or β-glucan uptake and processing were up-regulated in an S^0-independent manner. Most differentially transcribed open reading frames (ORFs) responding to S^0 in cellobiose-grown cells also responded to S^0 in maltose-grown cells; these ORFs included ORFs encoding a membrane-bound oxidoreductase complex (MBX) and two hypothetical proteins (PF2025 and PF2026). However, additional genes (242 genes; 108 genes were up-regulated and 134 genes were down-regulated) were differentially transcribed when S^0 was present in the medium of maltose-grown cells, indicating that there were different cellular responses to the two sugars. These results indicate that carbohydrate characteristics (e.g., glycoside linkage) have a major impact on S^0 metabolism and hydrogen production in *P. furiosus*. Furthermore, such issues need to be considered in designing and implementing metabolic strategies for production of biofuel by fermentative anaerobes.

Because of problems with sufficient access to petroleum and natural gas resources and the emerging threat of global warming, there is increasing interest in alternative energy options to supplement or replace fossil fuels (43). One prospect that has received considerable attention is the conversion of renewable resources (i.e., biomass) to ethanol using biological routes (20). While availability of bioprocess-based ethanol could offset current demands to some extent, problems with significant CO_2 emissions upon energy conversion would remain (37). A longer-term option being considered is the production of molecular hydrogen from biomass using fermentative, anaerobic microorganisms (38). For example, many mesophilic *Clostridium* and *Enterobacter* species can grow on fermentable sugars and produce hydrogen as a by-product of energy metabolism (8, 11, 16, 28, 38).

Studies suggest that biohydrogen production rates may be enhanced at higher temperatures (9, 23). In fact, the production and consumption of molecular hydrogen drive the microbial physiology and bioenergetics of many hyperthermophilic bacteria and archaea inhabiting hydrothermal environments (1). The potential of these microorganisms for biofuel processes has not gone unnoticed (25). Elevated processing temperatures could facilitate the breakdown of complex carbohydrates to fermentable sugars and, at the same time, minimize the impact of H_2-consuming mesophilic acetogens and methanogens associated with heterogeneous biomass feedstocks. Studies of H_2 production by a range of high-temperature bacteria and archaea, including *Thermotoga neapolitana* (58), *Caldicellulosiruptor saccharolyticus* (24, 57), *Pyrococcus furiosus* (46), and *Thermococcus kodakaraensis* KOD1 (25), have been reported. Notably, *P. furiosus* was found to have high specific hydrogen production rates when it was grown on maltose in a continuous bioreactor configuration (25, 46).

P. furiosus, a facultative sulfur-reducing, fermentative anaerobe, grows optimally at 98 to 100°C on sugars or peptides as the primary carbon and energy source, producing hydrogen, hydrogen sulfide (in the presence of elemental sulfur [S^0]), organic acids (primarily acetate when it is grown on sugars), and small amounts of alanine and ethanol (18, 46). The genesis of these products in the presence and absence of reduced inorganic sulfur species is key to understanding the bioenergetics of this microorganism, especially as it relates to sinks and sources of reductants. Three different hydrogenases from *P. furiosus* have been characterized; two are cytoplasmic (soluble hydrogenase 1 [SH1] and soluble hydrogenase 2 [SH2]) (34,

* Corresponding author. Mailing address: Department of Chemical and Biomolecular Engineering, North Carolina State University, EB-1, 911 Partners Way, Raleigh, NC 27695-7905. Phone: (919) 515-6396. Fax: (919) 515-3465. E-mail: rmkelly@eos.ncsu.edu.

‡ Present address: The Jackson Laboratory, 600 Main Street, Bar Harbor, ME 04609.

§ Present address: SAS Institute, Cary, NC.

¶ Present address: Wyeth Pharmaceuticals, Sanford, NC.

† Supplemental material for this article may be found at http://aem.asm.org/.

▽ Published ahead of print on 7 September 2007.

35), and one is membrane associated (MBH) (45). It has been suggested that the genome encodes a fourth hydrogenase designated MBX (52). However, this is not the case as DNA microarray analyses have shown that the *mbx* operon is up-regulated in S^0-grown cells, which do not produce hydrogen and lack measurable hydrogenase activity (2, 49).

Energy conservation in *P. furiosus* has been linked in part to hydrogen production by the ferredoxin-dependent MBH, which generates a proton gradient across the cellular membrane to drive ATP production (45). Reduced ferredoxin is generated by pyruvate oxidoreductase (POR), which also produces acetyl coenzyme A (acetyl-CoA) (32) that is used to generate acetate and ATP by acetyl-CoA synthetase (36). POR has also been connected to acetaldehyde formation from excess reductant accumulating in the cytoplasm (32). Acetaldehyde can be removed by an aldehyde oxidoreductase to regenerate reduced ferredoxin and acetate, but at the expense of losing the energy conserved as ATP in the acetyl-CoA pathway (5, 27, 42). Acetaldehyde could also be converted into ethanol by alcohol dehydrogenases (31, 54), but at the expense of reducing equivalents in the form of NADPH. This pathway makes ethanol a potential sink when cells are challenged with reductant overflow (33). Another reductant sink is alanine, which is generated from pyruvate by the coordinated action of glutamate dehydrogenase and alanine aminotransferase at the expense of NADPH (60). While other routes to alanine formation are possible, such routes are not apparent from the *P. furiosus* genome sequence. To reduce the amount of carbon entering the glycolytic pathway, *P. furiosus*, like other *Thermococcales*, can produce glycogen (21) and extracellular polysaccharides, which could in turn provide the basis for biofilm formation (40, 41).

Although much has been reported about the role of specific enzymes and proteins in the central metabolic pathways of *P. furiosus* (17, 44, 45), the mechanism of S^0 reduction and the impact of S^0 on this archaeon's bioenergetics are still not clear. Sulfur reduction proceeds through polysulfides produced by nucleophilic attack on elemental sulfur (6), but so far the mechanism of S^0 reduction has been studied only in maltose-grown cells. S^0-grown cells do not produce hydrogen (18), and preliminary transcriptional analysis showed that the three operons encoding the three hydrogenases are dramatically down-regulated in the presence of S^0 (49). Conversely, two operons, including the genes encoding MBX and two so-called sulfur-induced proteins (Sips), were up-regulated in S^0-grown cells and were proposed to play a key role in H_2S evolution (49). Additional transcriptional and biochemical analyses have confirmed these results and have also shown that CoA is involved in S^0 reduction (G. J. Schut and M. W. W. Adams, unpublished data).

Given the potential of *P. furiosus* as an H_2 producer, it is important to understand the intricacies of its bioenergetics with different types of biomass. Here, a whole-genome DNA microarray was used in conjunction with high-temperature chemostat experiments to further explore the connection between the utilization of two different types of carbohydrates, product formation, and the role that S^0 plays in cellular bioenergetics. Surprisingly, the two carbohydrates examined here (maltose and cellobiose) have very different impacts on the bioenergetics and on H_2 production.

MATERIALS AND METHODS

Growth and maintenance of *P. furiosus*. *P. furiosus* DSM3638 was routinely cultured anaerobically at 90°C on a sea salts-based medium supplemented with 1 g/liter yeast extract with or without S^0, as described previously (51). In brief, the base medium (950 ml) and yeast extract were autoclaved together, after which 50 ml of a membrane-filtered sugar solution (maltose or cellobiose obtained from Sigma, St. Louis, MO) or tryptone (Fisher Scientific, Pittsburgh, PA) was added at a final concentration of 3.3 g/liter. To achieve anaerobic conditions, the medium was first sparged with N_2. Then 0.6% (by volume) of a 10% sodium sulfide solution was added to the culture, which was sparged with N_2 again prior to inoculation.

Determination of product gas composition. The content of the exhaust gas was determined periodically by using a Gow-Mac G400C online gas chromatograph with a thermoconductivity detector (Gow-Mac, Bethlehem, PA); the H_2 content was determined with N_2 as the carrier gas, and the CO_2 and H_2S contents were determined with He as the carrier gas. The exhaust manifold was connected to a cooling tower to minimize water carryover from the heated bioreactor. Before entering the autosampler, the exhaust gas was dried by passage through an adsorber filled with Drierite (Fisher Scientific, Pittsburgh, PA). Results were recorded by using the Chromperfect 5.0 software (Justice Laboratory Software, Denville NJ), and the gas composition was calculated by comparing the peak area to calibration curves.

Continuous culture. The continuous culture bioreactor configuration used was similar to one described previously (39). The temperature of the reactor was measured with a type K thermocouple and controlled within ±1°C of the desired temperature by a Digi-Sense controller (Cole Palmer Instrument, Vernon Hills, IL) coupled to a heating mantle (Fisher Scientific, Pittsburgh, PA). The culture pH was monitored with an autoclavable pH probe and a Chemcadet pH controller (Cole Palmer Instrument, Vernon Hills, IL). The reactor was placed on a stir plate so that a Teflon stirring bar could be used for mixing. The inlet gas flow rate was controlled with a rotameter at 21 ml/min. N_2 or He (NWSCO, Charlotte, NC) was used to sparge the reactor. Product gases (H_2, H_2S, and CO_2) were determined by gas chromatography.

Prior to each set of experiments, *P. furiosus* was subcultured (four passages) from a stock in 125-ml serum bottles. Starter cultures (30 ml) were prepared and cooled to room temperature prior to inoculation of a 2-liter round-bottom flask with 1 liter (working volume) at an initial density of 6×10^6 cells/ml. After inoculation, the reactor was operated in batch mode for 6 h before continuous operation was initiated at a dilution rate of 0.15 h^{-1}. Once stabilized at 0.15 h^{-1} for 12 h, the dilution rate was increased to 0.45 h^{-1}. Samples for cell counting and product analysis were taken from the reactor every 2 h. The culture usually achieved steady state after three volume changes, so the final sample was usually harvested roughly 12 h after operation was initiated at a dilution rate of 0.45 h^{-1}. For sulfur-grown cultures, 5 g of elemental sulfur was added to the 1-liter culture at the start. To avoid S^0 limitation, 10 g of S^0 was added directly to the reactor through a port on the top after 4 h of operation at a dilution rate of 0.45 h^{-1}. In all cases, gas production profiles and exhaust gas concentrations were monitored to ensure that samples used for subsequent analysis were obtained under mechanical and biological steady states.

Determination of cell density and metabolites in spent medium. Cell densities were determined by epifluorescence microscopy (51). Samples (1 ml) were removed from the reactor and added to 100 μl of a 2.5% glutaraldehyde solution (Sigma, St. Louis, MO). Each mixture was vortexed briefly and let stand for 5 min. From this mixture, 5 to 20 μl was added to 4.9 ml of a 0.004% acridine orange solution, following which the solution containing stained cells was passed through a 25-mm black polycarbonate filter with a pore size of 0.22 μm (GE Water Process Technology, Minnetonka, MN). The filter was placed on a glass slide and examined using an epifluorescence microscope (Nikon, Melville, NY). Ten fields were counted for each sample and cell density. Residual sugar concentrations were determined by first hydrolyzing maltose with α-glucosidase (Roche Diagnostics, Basel, Switzerland) and cellobiose with β-glucosidase from *P. furiosus* (4). The glucose was then measured with a glucose assay kit (Sigma, St. Louis, MO). Acetate and ethanol concentrations were also determined with assay kits (R-Biopharm, Inc., Marshall, MI). Pyruvate was assayed by examining the oxidation of NADH (Sigma, St. Louis, MO) to NAD^+ in the presence of lactate dehydrogenase (Sigma, St. Louis, MO). The subsequent changes in the optical density at 340 nm were determined spectrophotometrically (Perkin-Elmer, Boston, MA).

Analysis of liquid phase fermentation products. An HPX-87H cation-exchange column and guard column (Bio-Rad Laboratories, Hercules, CA) were used to quantify the residual sugar and fermentative products by high-performance liquid chromatography (Waters Corp., Milford, MA). The mobile phase

TABLE 1. Bioenergetic parameters for *P. furiosus* growing in chemostat cultures on maltose, cellobiose, and tryptone in the presence and absence of S^0[a]

Substrate(s)	Cell density (10^8 cells/ml)	Total protein (mg/liter)	Q_S (mmol/g/h)	Q_A (mmol/g/h)	Q_{Ala} (mmol/g/h)	Q_E (mmol/g/h)	Q_{H2} (mmol/g/h)	Q_{H2S} (mmol/g/h)	Q_{CO2} (mmol/g/h)	Q_{H2+H2S} (mmol/g/h)	Doubling time for batch growth (min)
Maltose	2.0	37	24.7	24.5	8.2	ND	63.6	ND	34.8	63.6	80
Maltose + S^0	4.1	142	18.1	24.5	0.1	ND	ND	55.1	31.4	55.1	40
Cellobiose	2.4	66	25.0	37.1	5.2	2.9	94.6	ND	47.8	94.6	90
Cellobiose + S^0	3.1	84	19.8	26.1	4.0	2.3	43.6	17.9	30.1	61.5	50
Tryptone + S^0	2.4	122	NA	6.5	ND	ND	ND	46.6	25.1	46.6	42[b]

[a] Abbreviations: Q_S, specific rate of consumption of substrate per gram of protein; Q_A, specific rate of production of acetate per gram of protein; Q_{Ala}, specific rate of production of alanine per gram of protein; Q_E, specific rate of production of ethanol per gram of protein; Q_{H2}, specific rate of production of H_2 per gram of protein; Q_{H2S}, specific rate of production of H_2S per gram of protein; Q_{CO2}, specific rate of production of CO_2 per gram of protein; Q_{H+H2S}, combined specific rates of production of H_2 and H_2S; ND, not detected; NA, not applicable.
[b] Data from reference 50.

was a 0.008 N sulfuric acid solution, and the column temperature was maintained at 35°C. Standards composed of freshly prepared sea salts-based medium containing known amounts of maltose or cellobiose were injected and used to generate standard curves. Alanine concentrations were determined in culture supernatant samples separated on a Symmetry C_{18} reverse-phase column, using phenyl isothiocyanate derivatization (Pierce Biotechnology, Rockford, IL).

RNA isolation and purification. Cells from the reactor were harvested into a glass vessel in a dry ice-ethanol bath. Cells were separated from the spent medium by centrifugation at 10,000 × *g*. RNA extraction and purification were carried out as described previously (29, 50).

Microarray experiment and data analysis. RNA samples were converted to fluorescence-labeled cDNA and hybridized to a whole-genome *P. furiosus* microarray according to a modified protocol from TIGR (10). The amount of cDNA hybridized on a slide was normalized to minimize operational variations. Each slide was hybridized for 18 h, washed, and read (ScanExpress scanner; Perkin-Elmer, Boston, MA). Spot intensities were quantified by the vendor-supplied software, and quality control was confirmed by using MA plots (13) of raw intensity values. Raw intensities were normalized by using a mixed-effects analysis of variance model described previously (10). Data for Venn diagrams were generated by JMP software (SAS Institute, Cary, NC).

RESULTS

Influence of growth substrate and S^0 on the bioenergetics of chemostat-grown *P. furiosus*. Chemostat cultures grown at 90°C (dilution rate, 0.45 h^{-1}) were used to assess the influence of the carbon source and S^0 on the bioenergetics of *P. furiosus*. Tables 1 and 2 summarize the growth characteristics and stoichiometry for cultures grown on maltose or cellobiose in the presence and absence of S^0. Data for growth on tryptone (peptides) in the presence of S^0 are also included; no growth was observed on tryptone in the absence of S^0. The impact of glycoside linkage on *P. furiosus* growth and bioenergetics was profound. In the absence of S^0, the cell densities for growth on cellobiose or maltose were comparable, although cellobiose generated 50% more protein. Equivalent increases in acetate, CO_2, and H_2 production were also observed. While no ethanol was detected for growth on maltose, small amounts were measured for growth on cellobiose. As expected, the presence of S^0 in the medium of maltose-grown cells led to complete cessation of H_2 production; the H_2S levels were comparable to the H_2 levels in the absence of S^0. However, the protein production on a medium containing maltose and S^0 increased nearly fourfold, even in the face of reduced specific sugar consumption, compared to the protein production by S^0-free cells. Specific rates of production of acetate and CO_2 for growth on maltose were not affected by S^0. For cells grown on cellobiose in the presence of S^0, the cell density and protein yields were greater than the cell density and protein yields of cells grown in the absence of S^0, while the specific rates of CO_2 and acetate production decreased by one-third. Surprisingly, while H_2 production decreased in the presence of S^0, it decreased only by about 50% (from 94.6 to 43.6 mmol/g cell protein/h) and did not decrease to zero, as observed with cells grown on maltose plus S^0. The effect of S^0 on maltose-grown cells was more profound than the effect of S^0 on cellobiose-grown cells. Compared to a culture grown with maltose plus S^0 or with cellobiose plus S^0, the culture grown with tryptone plus S^0 had a much lower cell density but comparable protein production levels. This comparison also showed that much less acetate and slightly less CO_2 were produced in the culture grown with tryptone plus S^0. No H_2 could be detected in cultures grown on tryptone plus S^0.

Table 2 shows the growth stoichiometry of *P. furiosus*, based on information in Table 1. The theoretical amounts of primary metabolic products are 4, 2, and 2 mol/mol of glucose equivalents consumed for H_2 (or H_2 plus H_2S), acetate, and CO_2, respectively. For maltose-grown cells, the amounts of acetate,

TABLE 2. Stoichiometry of *P. furiosus* conversion of growth substrates[a]

Substrate(s)	$Y_{X/S}$ (mg protein/mmol sugar consumed)	Q_A/Q_S	Q_E/Q_S	Q_{CO2}/Q_S	Q_{H2+H2S}/Q_S	Q_{CO2}/Q_A	Q_{H2+H2S}/Q_{CO2}
Theoretical		2	0	2	4	1	2
Maltose	37	1.0	0	1.4	2.6	1.4	1.8
Maltose + S^0	50	1.4	0	1.7	3.0	1.3	1.8
Cellobiose	36	1.5	0.1	1.9	3.8	1.3	2.0
Cellobiose + S^0	46	1.3	0.1	1.5	3.1	1.2	2.1
Tryptone + S^0	NA	NA	NA	NA	NA	3.8	1.9

[a] $Y_{X/S}$, apparent yield coefficient. For other abbreviations, see Table 1, footnote *a*.

CO_2, and H_2 (per mole of glucose) were close to the values reported previously (46). The results shown in Table 2 indicate that there were significant differences in the ways in which cellobiose and maltose were metabolized. For example, the largest amount of H_2 was produced by the cellobiose-grown culture, which had a ratio of the specific rate of production of H_2 (Q_{H2}) to the specific rate of consumption of glucose (Q_S) of 3.8. This is close to the theoretical maximum of 4, suggesting that most of the carbon flux from the sugar substrate was directed to acetate formation, which resulted in higher hydrogen levels.

In contrast, maltose-grown cultures produced only 70% as much H_2, with a Q_{H2}/Q_S value of 2.6. With both sugars, the presence of S^0 resulted in comparable ratios of the combined specific rates of production of H_2 plus H_2S (Q_{H2+H2S}) to Q_S (3.0 to 3.1) which were intermediate between the values obtained with cellobiose alone and with maltose alone. Consequently, S^0 appears to have opposite effects on the metabolism of the two sugars. Its presence in cellobiose-grown cultures decreased the amount of carbon that was diverted to acetate formation (lower Q_{H2+H2S}/Q_S value and lower ratio of the specific rate of production of acetate [Q_A] to Q_S with S^0), while more carbon derived from sugar was diverted to acetate formation in maltose-grown cells when S^0 was added (higher Q_{H2+H2S}/Q_S and Q_A/Q_S values with S^0).

Cells grown with only maltose have been reported to dispose of excess carbon as alanine (41). Here, the specific rate of accumulation of alanine (Q_{Ala}) was higher in a maltose-grown culture than in a cellobiose-grown culture (8.2 versus 5.2 mmol/g/h). Q_{Ala}/Q_A was approximately 0.33 in the maltose-grown culture and 0.14 in the cellobiose-grown culture. However, addition of S^0 to the maltose-grown culture eliminated alanine production. The impact of S^0 on alanine accumulation in a cellobiose-grown culture was not significant as the ratio of Q_{Ala} to Q_A did not change (0.15). These results suggest that maltose-grown cells diverted some carbon flux into alanine and consequently reduced the amount of pyruvate processed via POR; the alanine production in a cellobiose-grown culture, on the other hand, was not affected significantly by addition of S^0.

Some ethanol was produced in cellobiose-grown cells (with and without S^0) (Table 1), presumably from acetaldehyde by using alcohol dehydrogenases and NADPH (31). However, the amounts represent less that 5% of the H_2 and H_2S produced (in terms of reductant equivalents), ruling out the possibility that ethanol is a major electron sink. Ethanol formation presumably provides a means for removing potentially toxic acetaldehyde generated as a by-product by POR in a highly reducing environment (33), although why this should be necessary in cellobiose-grown cells rather than maltose-grown cells is not clear. Extracellular pyruvate was not detected in any of the culture supernatants.

Global effect of glycoside linkage and S^0 on the *P. furiosus* transcriptome. A whole-genome cDNA microarray was used to assess the transcriptional response of *P. furiosus* during growth on the two sugars both with and without S^0. Sets of regulated genes that were common to or unique to the five growth conditions were separated into glycoside, sulfur, and peptide effects, and the results are summarized in Fig. 1.

Glycoside effect. The glycoside effect is shown in Fig. 1a. In cells grown on cellobiose compared to cells grown on maltose,

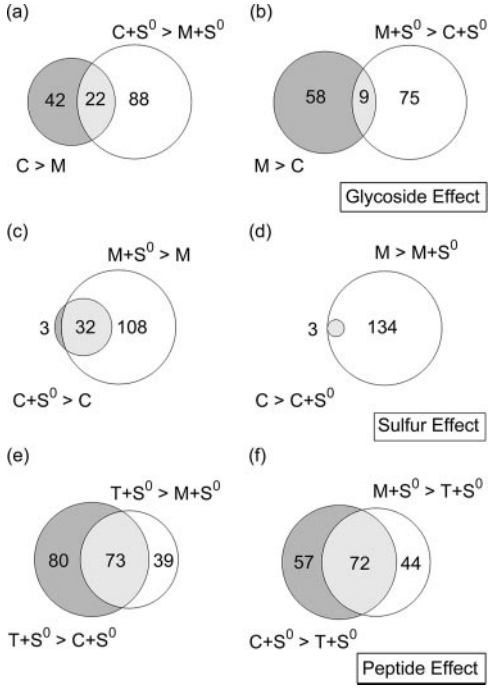

FIG. 1. Venn diagram analysis showing the numbers of genes regulated twofold or more (a) on cellobiose (C) (C and C+S^0) compared to maltose (M) (M and M+S^0), (b) on maltose (M and M+S^0) compared to cellobiose (C and C+S^0), (c and d) in the presence of S^0, and (e and f) on tryptone (T) plus S^0 (T+S^0). For example, in panel a, 64 genes (in the absence of S^0) and 110 genes (in the presence of S^0) were up-regulated twofold or more on cellobiose compared to maltose; 22 genes were common to both comparisons. See Tables 2 to 4 and the supplemental material for the complete lists.

152 genes were up-regulated, 64 genes in the absence of S^0 and 110 genes in the presence of S^0; of this group, 22 genes were differentially transcribed independent of the presence of S^0. On maltose compared to cellobiose, 141 genes were induced, 67 in the absence of S^0 and 84 genes in the maltose-plus-S^0 versus cellobiose-plus-S^0 contrast. Of these 141 genes, only 9 were differentially transcribed independent of the presence of S^0.

Sulfur effect. The presence of elemental sulfur had a profound effect on the transcriptome of maltose-grown cells; the effect on these cells was much greater in terms of the number of open reading frames (ORFs) affected than the effect on cellobiose-grown cells. All but three of the differentially transcribed ORFs responding to S^0 in cellobiose-grown cells (35 ORFs were up-regulated and 3 ORFs were down-regulated) also responded to S^0 in maltose-grown cells. However, 277 genes were differentially transcribed (140 genes were up-regulated and 137 genes were down-regulated) when S^0 was added to maltose. This difference in the magnitude of the transcriptional response for S^0-based growth on the two sugars is presumably reflected in the bioenergetic parameters listed in Tables 1 and 2. The dramatic bioenergetic impact of S^0 on maltose-grown cells compared to cellobiose-grown cells in terms of cell density, protein production, elimination of H_2 production with concomitant H_2S production, and alanine pro-

duction indicates that there is a fundamental difference in how the two sugars are metabolized.

Peptide effect. The tryptone-plus-S^0 versus sugar-plus-S^0 transcriptional contrast was independent of glucoside linkage (see the supplemental material). For the comparison of cells grown with tryptone plus S^0 and cells grown with cellobiose plus S^0, 282 genes were differentially transcribed (153 genes were up-regulated and 129 genes were down-regulated), while for the comparison of cells grown with tryptone plus S^0 and cells grown with maltose and S^0, 228 genes were affected (112 genes were up-regulated and 116 genes were down-regulated). When tryptone was compared to the sugars, there were 145 differentially transcribed genes in common (73 genes were up-regulated and 72 genes were down-regulated.

Cellobiose transcriptome. Table 3 lists genes (Fig. 1) that were up-regulated in *P. furiosus* grown on cellobiose with and without S^0 but whose expression was not significantly changed in maltose- or peptide-grown cells (with or without S^0). Genes located in the corresponding genome neighborhoods are also listed. The cellobiose-affected genes included PF0496, encoding a transcriptional regulator related to the maltose/maltodextrin-regulated TrmB (30); β-glucan processing loci (PF0073 to PF0076), which encode two glycoside hydrolases (PF0073 [59] and PF0076 [56]); and genes encoding two alcohol dehydrogenases (PF0074 [31] and PF0075 [54]), which are assumed to be involved in acetaldehyde conversion to ethanol. Two putative ABC transporter binding proteins (PF0360 and PF0361) previously shown to be up-regulated during growth on chitin (19) but perhaps more likely involved in cellobiose transport responded, as did PF1696 and PF1697, encoding components of a putative ABC transporter, indicating a possible role in cellobiose uptake. Several genes related to capsular polysaccharide synthesis (PF0765 to PF0768, PF0776, and PF0777) were up-regulated, which may be related to the higher turbidity of cellobiose-grown cultures than of cultures grown on maltose (data not shown). It was interesting that PF1206-PF1207, a VapBC toxin-antitoxin locus was up-regulated, apparently in concert with up-regulation of PF1208, encoding a β-mannosidase/β-glucosidase (4). While VapBC toxin-antitoxin loci respond to heat shock in the hyperthermophile *Sulfolobus solfataricus* (53), this is the first indication that this system may be involved in metabolic regulation under nonstress conditions.

Maltose transcriptome. Table 4 lists selected genes (Fig. 1) that were up-regulated in *P. furiosus* grown on maltose (with and without S^0) compared to all other conditions. The transcriptional profiles of genes affected by maltose, including those belonging to the Mal II operon (D. A. Comfort and R. M. Kelly, unpublished data), are also listed for comparison. In addition, the presence of S^0 affected the regulation of α-glucan-related genes differently for the two sugars. For example, PF0477 encodes an extracellular α-amylase involved in starch hydrolysis (29). Its expression was up-regulated ninefold when cells grown with maltose were compared with cells grown with cellobiose but was down-regulated fivefold when cells grown with maltose plus S^0 were compared with cells grown with cellobiose plus S^0 and threefold when cells grown with maltose plus S^0 were compared with cells grown with tryptone plus S^0. This type of response was noted previously for growth on tryptone (29, 48). The Mal I operon (PF1739 to PF1749) (62), which includes genes encoding an ABC trehalose/maltose transporter (PF1739 to PF1741) and a TrmB homolog (PF1743) known to regulate maltose uptake (30), was minimally affected by the presence of maltose. This may have been due in part to small amounts of trehalose present in yeast extract, which caused this operon to be transcribed under all growth conditions tested. It was interesting that the Mal II operon (PF1933 to PF1939) did not respond to glucoside linkage when S^0 was present. A similar trend was observed for PF1109 and PF1110, which encode a single extracellular protein that binds to starch (C.J. Chou and R. M. Kelly, unpublished data) and is predicted to contain CBD9 domains (29).

The difference in transcription patterns between the different operons that encode maltose-processing enzymes may be related to other aspects of maltose assimilation (29). Maltose can be converted to glucose and maltotriose by α-glucanotransferase (PF0272), and the glucose is subsequently phosphorylated to glucose-1-phosphate by α-glucanophosphorylase (PF1535). Glucose-1-phosphate can then be converted into glucose-6-phosphate by phosphoglucomutase (PF0588) (3) or directed into polysaccharide biosynthesis (40). PF0272 was significantly up-regulated by maltose in all comparisons, especially in the presence of S^0. On the other hand, the α-glucanophosphorylase operon (PF1535 to PF1537) was up-regulated most in the presence of S^0, implying that S^0 has an impact on the mechanisms by which maltose is taken into the cell. Alternatively, maltose can be hydrolyzed into glucose by a novel isomaltase (PF0132) (12) (Comfort and Kelly, unpublished data) and converted to glucose-6-phosphate by an ADP-dependent glucokinase (PF0312) (26). The transcription level of PF0132 was constitutively high under all conditions but was extraordinarily high in the culture containing only maltose. However, PF0312 and PF0588, which control the influx to the glycolytic pathway, responded indifferently to maltose and cellobiose but were down-regulated on tryptone (peptides); similar profiles were observed for other intermediate glycolytic genes (see below). Genes encoding several stress proteins were up-regulated on maltose compared with cellobiose (with and without S^0), including PF0126, encoding a Rad25 DNA repair protein (61); PF0347, encoding an unknown hypothetical protein proximate to the detoxification enzyme aldehyde oxidoreductase (27); PF0456, encoding a Zn-dependent carboxypeptidase reportedly responsive to heat shock (51); and PF0505, encoding a hypothetical protein next to a DNA helicase, implicated in DNA repair. PF0090 encodes an *S*-adenosylmethionine-dependent tungsten cofactor biosynthesis protein, and the elevated expression level may indicate that there is an increased demand of tungsten-containing aldehyde oxidoreductases essential for cellular detoxification (5).

Peptide transcriptome. Table 5 lists selected genes that responded to tryptone as a carbon and energy source. Only those genes associated with glycolytic and gluconeogenesis pathways are included; amino acid anabolism genes are listed in tables in the supplemental material. The peptide transcriptome analysis was consistent with previous transcriptional response analyses comparing maltose- and peptide-grown *P. furiosus* in batch culture (48). In contrast to sugars, tryptone (peptides) induced transcription of genes involved in gluconeogenesis (PF0613, PF0289, and PF1874), oligopeptide transport (PF0191 to PF0195), energy conservation via acyl-CoA (PF0233, PF0532, and PF1838), fatty acid metabolism (PF0972 to PF0974), and

TABLE 3. Transcriptional responses of selected ORFs to β-glycoside linkage (cellobiose) independent of S^0 in *P. furiosus*

Function	GeneID no.	Transcriptional response (fold change)[a]			Annotation
		Cellobiose vs maltose	Cellobiose + S^0 vs maltose + S^0	Cellobiose + S^0 vs tryptone + S^0	
Cellobiose hydrolysis	PF0073	35.5	22.7	8.0	β-Glucosidase
	PF0074	7.9	8.4	4.8	Alcohol dehydrogenase, short chain
	PF0075	14.5	12.5	6.3	Alcohol dehydrogenase, class IV
	PF0076	2.6	2.2	2.2	β-1,3-Endoglucanase
Chitin transport and utilization	PF0355	NC	NC	NC	VapC1
	PF0355.1	NA	NA	NA	VapB1
	PF0356	NC	NC	NC	GH1, β-glycosidase
	PF0357	NC	NC	NC	ABC transporter, binding protein
	PF0358	NC	NC	NC	ABC transporter, permease
	PF0359	NC	NC	NC	ABC transporter, permease
	PF0360	7.7	11.3	6.2	ABC transporter, ATP-binding protein
	PF0361	4.6	7.9	4.9	ABC transporter, ATP-binding protein
	PF0362	NC	NC	NC	Glucosamine–fructose-6-phosphate aminotransferase
	PF0363	NC	NC	NC	Exo-β-D-glucosaminidase
Transport	PF0429	2.9	3.9	6.1	NA^+/proline symporter
Carbohydrate utilization	PF0496	3.2	2.2	2.8	Transcriptional regulator, TrmB homolog
Gluconeogenesis	PF0613	2.9	2.4	3.1 ↓	Archaeal fructose 1,6-bisphosphatase
Polysaccharide synthesis	PF0765	5.9	18.4	6.0	UDP-*N*-acetyl-D-mannosaminuronate dehydrogenase
	PF0766	3.3	8.1	4.4	Dehydrogenase
	PF0767	4.8	13.5	5.3	Aspartate aminotransferase
	PF0768	4.6	11.9	4.5	Acetyltransferase
Regulation/polysaccharide anabolism	PF0776	2.2	3.8	4.6	Nucleic acid-binding protein, PIN domain
	PF0777	4.3	8.8	7.9	Capsular polysaccharide biosynthesis
β-Glucan uptake	PF1206	2.4	1.6	1.6	VapC12 toxin
	PF1207	5.2	5.0	3.9	VapB12 antitoxin
	PF1208	12.5	8.5	5.5	β-Mannosidase
	PF1209	NC	NC	NC	ABC transporter, binding protein
	PF1210	NC	NC	NC	ABC transporter, permease
	PF1211	2.4	3.1 ↓	3.0	ABC transporter, permease
	PF1212	NC	NC	NC	ABC transporter, uptake protein
	PF1213	NC	NC	NC	ABC transporter, binding protein
Cofactor biosynthesis	PF1674	7.4	12.0	5.3	Protein-tyrosine phosphatase
	PF1675	NC	NC	2.0 ↓	Aspartate racemase
	PF1676	9.6	19.4	8.3	Biotin-(acetyl-CoA carboxylase) ligase
Sugar transport	PF1695	NC	NC	NC	ABC transporter, binding protein
	PF1696	15.2	34.1	10.7	ABC transporter, ATPase
	PF1697	9.4	45.3	7.7	ABC transporter, permease
	PF1698	NC	NC	NC	ABC transporter, permease

[a] NC, no change (≤1.5-fold change); NA, not available; ↓, down-regulated.

keto acid catabolism (PF0533 to PF0534 and PF1767 to 1773). On the other hand, genes involved in glycolysis (PF0215, PF0312, PF1784, PF1956, and PF1959), amino acid anabolism, and de novo purine synthesis (see the supplemental material) were down-regulated by tryptone. The tungsten-containing aldehyde oxidoreductase, WOR5 (PF1480), was also down-regulated by tryptone. The concerted down-regulation of amino acid catabolic genes and up-regulation of amino acid anabo-

TABLE 4. Transcriptional responses of selected ORFs to α-glycoside linkage (maltose) independent of S^0 in *P. furiosus*

Function	GeneID no.	Transcriptional response (fold change)[a]			Annotation
		Maltose vs cellobiose	Maltose + S^0 vs cellobiose + S^0	Maltose + S^0 vs tryptone + S^0	
Glucan hydrolysis	PF0477	8.9	4.9 ↓	3.2 ↓	Extracellular α-amylase
	PF0478	NC	1.7	2.5	Cycloglucantransferase
	PF1109	3.5	NC	5.8	Extracellular protein, putative amylase
	PF1110	3.3	NC	5.1	Extracellular protein
Glucokinase pathway	PF0132	3.0	NC	1.7	Isomaltase
	PF0133	1.6	1.7	2.0	Hypothetical protein
	PF0312	1.6 ↓	NC	2.4	ADP-dependent glucokinase
Phosphorylation pathway	PF0272	12.1	18.1	21.4	4-α-Glucanotransferase
	PF0588	NC	1.6	1.9	Phosphoglucose mutase
	PF1535	1.6	2.8	3.9	Glucanophosphorylase
	PF1536	NC	2.5	3.7	ADP-ribose binding module
	PF1537	1.7	2.5	3.3	Membrane protein, DUF835
Mal I operon	PF1739	1.6	2.1	1.5 ↓	Trehalose/maltose binding protein
	PF1740	NC	NC	2.0 ↓	Trehalose/maltose transport, permease
	PF1741	NC	1.8	1.9 ↓	Trehalose/maltose transport, permease
	PF1742	1.7	1.9	NC	Putative trehalose synthase
	PF1743	1.8	2.0	NC	TrmB
	PF1744	1.6	2.0	1.6 ↓	Trehalose/maltose transport, ATPase
	PF1745	NC	1.6	NC	L-Fructose isomerase
	PF1746	NC	1.6	1.8 ↓	Glycogen debranching enzyme
	PF1747	NC	NC	2.0 ↓	Hypothetical protein, DUF377
	PF1748	1.9	1.7	NC	Putative sulfate transport, permease
	PF1749	NC	1.6	NC	Putative sulfate transport, permease
Mal II operon	PF1933	3.9	NC	NC	Maltodextrin transport, ATPase
	PF1934	8.3	NC	1.9	Amylopullulanase, C-terminal
	PF1935	8.4	NC	2.2	Amylopullulanase, N-terminal
	PF1936	8.1	NC	1.9	Maltodextrin transport, permease
	PF1937	NC	2.1	2.8	Maltodextrin transport, permease
	PF1938	9.1	NC	2.9	Maltodextrin binding protein (MalE-like)
	PF1939	NC	NC	NC	Intracellular cyclodextrinase, neopullulanase
Stress response	PF0090	2.0	4.5	2.2	Tungsten cofactor biosynthesis protein
	PF0126	6.2	6.5	NC	DNA repair protein Rad25
	PF0347	3.6	2.1	1.6 ↓	Next to aldehyde oxidoreductase
	PF0456	2.4	2.2	2.1 ↓	Carboxypeptidase, heat shock response
	PF0505	2.1	3.6	NC	Helix-turn-helix domain, next to DNA helicase
Unknown	PF0560	3.3	2.2	NC	Hypothetical protein
	PF0561	2.8	NC	NC	Hypothetical protein
	PF0962	3.0	2.1	1.7	Contains signal peptide
	PF1344	3.0	2.7	4.9	Putative maleate *cis-trans* isomerase

[a] NC, no change (≤1.5-fold change); NA, not available; ↓, down-regulated.

lism genes on both maltose plus S^0 and cellobiose plus S^0 indicated that the surge of biomass production on maltose plus S^0 may not be a direct result of utilizing peptide as a fermentation substrate, as previously suggested (2).

Sulfur transcriptome. Table 6 lists genes showing significant up-regulation in both maltose- and cellobiose-grown cells in the presence of S^0. Almost all genes regulated by S^0 in cellobiose-grown cultures were also present in the data set for cells grown with maltose plus S^0. These genes included several purine biosynthesis genes, most members of the membrane-bound oxidoreductase operon, genes encoding MBX (PF1441 to PF1454), and three members of the MBH operon (PF1433 to PF1435). The up-regulation of purine biosynthesis genes was likely the direct result of higher protein production stimulated by S^0. Two so-called sulfur-induced proteins, SipA (PF2025) and SipB (PF2026), were up-regulated by S^0, consistent with previous reports (49). The fact that SipA and SipB were up-regulated to a much greater extent by S^0 on maltose (101- and 22.9-fold, respectively) than on cellobiose (12.5- and 5.7-fold, respectively) suggests that there is a prominent bioenergetic role for these proteins in *P. furiosus* growing on the maltose.

Figure 2 summarizes the expression levels (based on least-squares mean estimates from analysis of variance mixed model analysis) of genes related to energy conservation. The two cytoplasmic hydrogenases in the *P. furiosus* genome, SH1 and SH2, are encoded by PF0891 to PF0894 and PF1329 to PF1332, respectively. In all cases, the transcription levels of

TABLE 5. Transcriptional responses of selected ORFs significantly regulated by tryptone independent of glycoside type in *P. furiosus*

Function	GeneID no.	Transcriptional response (fold change)[a]		Annotation[b]
		Tryptose + S^0 vs cellobiose + S^0	Tryptone + S^0 vs maltose + S^0	
Gluconeogenesis	PF0613	3.1	7.3	Fructose-1,6-bisphosphatase
	PF0289	2.6	3.1	Phosphoenolpyruvate carboxykinase
	PF1874	4.4	5.7	Glyceraldehyde-3-phosphate dehydrogenase
Transcriptional regulation	PF0054	2.6	2.2	Regulator, Lrp/AsnC family
	PF0055	3.5	2.2	Putative HTH transcription regulator
	PF0056	2.1	2.2	Putative carbohydrate binding protein
Aminotransferase	PF0121	3.1	2.6	Aromatic amino acid aminotransferase
	PF1497	3.4	2.2	Alanine aminotransferase
Oligopeptide ABC transporter	PF0191	5.4	11.2	Oligopeptide transporter, permease
	PF0192	4.7	9.6	Oligopeptide transporter, permease
	PF0193	4.5	10.6	Oligopeptide transporter, ATPase
	PF0194	3.6	8.1	Oligopeptide transporter, ATPase
	PF0195	5.6	8.6	Hypothetical protein
Acyl-CoA synthetase II	PF0233	2.8	2.3	Acyl-CoA synthetase II homolog
	PF1838	3.0	2.4	Acyl-CoA synthetase II homolog
	PF0532	2.2	2.4	Acyl-CoA synthetase II
Acetyl-CoA synthase	PF0972	3.5	7.5	Acyl carrier protein synthase
	PF0973	3.2	6.3	Acetyl-CoA synthase
	PF0974	3.3	7.8	Hypothetical protein
2-Keto acid ferredoxin oxidoreductase	PF0533	2.0	1.6	IOR, alpha subunit
	PF0534	2.1	2.0	IOR, beta subunit
	PF1767	15.0	10.8	KGOR, delta subunit
	PF1768	14.2	10.5	KGOR, gamma subunit
	PF1769	15.2	11.0	KGOR, beta subunit
	PF1770	12.7	9.6	KGOR, alpha subunit
	PF1771	12.9	8.9	KOR, alpha subunit
	PF1772	9.1	7.6	KOR, beta subunit
	PF1773	9.3	7.9	KOR, gamma subunit
Glycolysis	PF0215	2.1 ↓	3.0 ↓	Enolase
	PF0312	2.3 ↓	2.4 ↓	ADP-dependent glucokinase
	PF1784	2.3 ↓	2.7 ↓	ADP-dependent phosphofructokinase
	PF1956	2.1 ↓	2.6 ↓	Fructose-1,6-bisphosphate aldolase
	PF1959	2.2 ↓	3.3 ↓	Phosphoglycerate mutase,
Glutamate metabolism	PF0201	3.4 ↓	2.4 ↓	Aconitase
	PF0202	3.7 ↓	2.1 ↓	Isocitrate dehydrogenase
	PF0203	5.8 ↓	4.0 ↓	Citrate synthase
	PF0204	2.8 ↓	3.6 ↓	Glutamate synthase domain 1
	PF0205	4.1 ↓	5.8 ↓	Glutamate synthase domain 2
	PF0206	2.9 ↓	3.2 ↓	Glutamate synthase domain 3
	PF0207	2.1 ↓	2.3 ↓	Argininosuccinate synthase
	PF0450	35.9 ↓	25.2 ↓	Glutamine synthetase
	PF1602	4.2	NC	Glutamate dehydrogenase
	PF1852	1.9 ↓	6.6 ↓	Glutamate synthase small subunit
WOR5	PF1480	5.2 ↓	4.7 ↓	Aldehyde:ferredoxin oxidoreductase
Cofactor biosynthesis	PF1528	2.1 ↓	3.3 ↓	Predicted glutamine amidotransferase
	PF1529	3.5 ↓	5.9 ↓	Pyridoxine biosynthesis enzyme

[a] NC, no change (≤1.5-fold change); NA, not available; ↓, down-regulated.
[b] HTH, helix-turn-helix; IOR, indolepyruvate ferredoxin oxidoreductase; KGOR, 2-ketoglutarate ferredoxin oxidoreductase; KOR, 2-ketoacid ferredoxin oxidoreductase.

SH2 (PF1329 to PF1332) were similar, while transcription of SH1 (PF0891 to PF0894) was significantly down-regulated on maltose plus S^0 and tryptone plus S^0. These results support previous reports indicating that the presence of S^0 represses expression of SH1 in maltose-grown cultures, although expression of SH2 was also down-regulated under the same conditions (49). However, expression of SH1 was not down-regulated by S^0 in cellobiose-grown cultures. Silva et al. (52) and

TABLE 6. Transcriptional responses of selected ORFs to S^0 independent of glycoside type in *P. furiosus*

Function	GeneID no.	Transcriptional response (fold change)[a]		Annotation[b]
		Cellobiose + S^0 vs cellobiose	Maltose + S^0 vs maltose	
Purine metabolism	PF0153	4.1	2.1	SAICAR synthase
	PF0154	2.5	2.3	Glutamine phosphoribosylpyrophosphate amidotransferase
	PF0426	4.3	4.0	NCAIR synthetase
	PF1516	2.3	2.4	GMP synthase, PP-ATPase domain/subunit
	PF1517	4.8	3.1	Hypothetical protein
Transposon	PF1366	4.1	2.0	Transposase and inactivated derivatives
MBH membrane-bound hydrogenase	PF1433	12.2	7.1	MbhK (NADH dehydrogenase subunit NuoC)
	PF1434	11.0	6.7	MbhL (Ni-Fe hydrogenase, NuoD)
	PF1435	11.6	7.2	MbhM (NADH dehydrogenase subunit NuoH)
MBX membrane-bound oxidoreductase	PF1441	9.7	7.7	MbxN (four-cysteine proximal Fe-S binding protein)
	PF1442	8.0	6.1	MbxL (Ni-Fe hydrogenase, NuoD homolog)
	PF1443	8.7	6.1	MbxK (NADH dehydrogenase subunit NuoC)
	PF1444	9.0	6.2	MbxJ (four-cysteine proximal Fe-S binding protein)
	PF1445	9.9	7.9	MbxM (NADH dehydrogenase subunit NuoH)
	PF1446	5.5	5.0	MbxH′ (NADH dehydrogenase subunit NuoL)
	PF1448	7.3	4.7	MbxG (membrane-bound hydrogenase, anchoring structure subunit)
	PF1450	3.3	2.5	MbxD (membrane-bound hydrogenase, anchoring structure subunit)
	PF1451	7.6	5.4	MbxC (membrane-bound hydrogenase, anchoring structure subunit)
	PF1452	6.0	4.1	MbxB (membrane-bound hydrogenase, anchoring structure subunit)
Sulfur-induced protein	PF2025	12.5	101	SipA
	PF2026	5.7	22.9	SipB

[a] NC, no change (≤1.5-fold change); NA, not available.
[b] SAICAR, phosphoribosylaminoimidazole-succinocarboxamide synthase; NCAIR, phosphoribosylaminoimidazole carboxylase, ATPase subunit.

van Haaster et al. (55) suggested that SH1 and SH2 in *P. furiosus* serve as safety valves and recycling pathways for the H_2 that is produced (by MBH), such that SH1 may be responsive to cellular redox status, while SH2 provides a constitutive basal capacity for these functions. The membrane-bound hydrogenase MBH (PF1423 to PF1436) and the membrane-bound oxidoreductase MBX (PF1441 to PF1453) appeared to be reciprocally regulated. While many components of MBX were positively S^0 responsive, genes encoding MBH were downregulated by S^0 (Fig. 2), as previously reported for maltose-grown cells (49). This is consistent with the reciprocal regulation of MBH and MBX that occurs within minutes of addition of S^0 to *P. furiosus* cells growing on maltose (Schut and Adams, unpublished). Similarly, contrasting transcriptional responses of MBH and MBX were also noted in response to exposure of *P. furiosus* to gamma irradiation (61). However, the impact of S^0 on MBH expression during growth on cellobiose was much less than that during growth on maltose. This correlates with the gas profiles; H_2 production, which occurs via MBH, was measured in cells grown on cellobiose plus S^0 but not in cells grown on maltose plus S^0 (Tables 1 and 2). These data indicate that there is a close association of MBH with H_2 production and a close association of MBX with H_2S production on both sugars, not just in maltose-grown cells (49). Furthermore, the pattern of regulation of SipA (PF2025) and SipB (PF2026) was similar to that of many MBX components. This is consistent with the proposal (49) that these proteins are intimately involved in the H_2S production process rather than in the disposal of excess reducing equivalents through H_2 generation.

DISCUSSION

To achieve the goal of optimizing hyperthermophilic H_2 production and designing metabolic engineering strategies, it is crucial to understand the physiology and regulation of hydrogenesis at high temperatures, especially as this relates to processing carbon and energy sources. Here, an anaerobic chemostat was used to obtain bioenergetics parameters and profiles of key metabolites related to the transcriptome of *P. furiosus*. This information is summarized in Fig. 3.

It was interesting that in the absence of S^0, growth on maltose generated much less H_2 than growth on cellobiose, despite comparable specific sugar consumption rates on the two sugars. In *P. furiosus*, maltose can enter the glycolytic pathway via both ADP-glucokinase (PF0312) and glucanophosphorylase (PF1535). The maltose-only transcriptome showed that relevant hydrolases and transporters were induced by this sugar substrate, although genes involved in downstream hydrogenesis pathway were not. This suggests that maltose-only cultures may have a bottleneck, leading to lower protein production

C	C+S^0	M	M+S^0	T+S^0	Gene ID	Function
Ferredoxin						
					PF0096	Ferredoxin homolog
					PF0729	Ferredoxin homolog
					PF1909	Ferredoxin
Ferredoxin-NADP oxidoreductase						
					PF1327	FNOR homolog SudA
					PF1328	FNOR homolog SudB
					PF1910	FNOR homolog SudX
					PF1911	FNOR homolog SudY
Soluble hydrogenases						
					PF0891	Soluble Hydrogenase I beta
					PF0892	Soluble Hydrogenase I gamma
					PF0893	Soluble Hydrogenase I delta
					PF0894	Soluble Hydrogenase I alpha
					PF1329	Soluble Hydrogenase II beta
					PF1330	Soluble Hydrogenase II gamma
					PF1331	Soluble Hydrogenase II delta
					PF1332	Soluble Hydrogenase II alpha
Hydrogenase maturation factor						
					PF0559	Hydrogenase maturation factor
Membrane bound hydrogenase complex, MBH						
					PF1423	MbhA
					PF1424	MbhB
					PF1425	MbhC
					PF1426	MbhD
					PF1427	MbhE
					PF1428	MbhF
					PF1429	MbhG
					PF1430	MbhH
					PF1431	MbhI
					PF1432	MbhJ
					PF1433	MbhK
					PF1434	MbhL
					PF1435	MbhM
					PF1436	MbhN
					PF1437	CysH
Membrane bound oxidoreductase complex, MBX						
					PF1441	MbxN
					PF1442	MbxL
					PF1443	MbxK
					PF1444	MbxJ
					PF1445	MbxM
					PF1446	MbxH'
					PF1447	MbxH
					PF1448	MbxG
					PF1449	MbxF
					PF1450	MbxD
					PF1451	MbxC
					PF1452	MbxB
					PF1453	MbxA
					PF1454	Predicted Fe-S oxidoreductases
					PF1455	Small unidentified protein
					PF1456	Histone acetyltransferase HPA2 andrelated
					PF1457	Thiol-disulfide isomerase and thioredoxins
ABC type Iron-sulfur cluster transporter						
					PF1285	SufB
					PF1286	SufB
					PF1287	SufC
Sulfur induced protein, Nif B homologs						
					PF2025	SipA
					PF2026	SipB
Alcohol dehydrogenase						
					PF0074	ADH
					PF0075	ADH
Aldehyde oxidoreductase						
					PF0346	AOR
					PF1480	WOR5
					PF1961	WOR4

FIG. 2. Heat plot based on the least-squares means (mixed model analysis) of selected genes involved in energy conservation in *P. furiosus* grown on cellobiose (C), maltose (M), cellobiose plus S^0 (C+S^0), maltose plus S^0 (M+S^0), and tryptone plus S^0 (T+S^0). Open boxes indicate the highest expression levels, while dark gray boxes indicate the lowest expression levels. FNOR, ferredoxin NADPH oxidoreductase; ADH, alcohol dehydrogenase; AOR, aldehyde oxidoreductase.

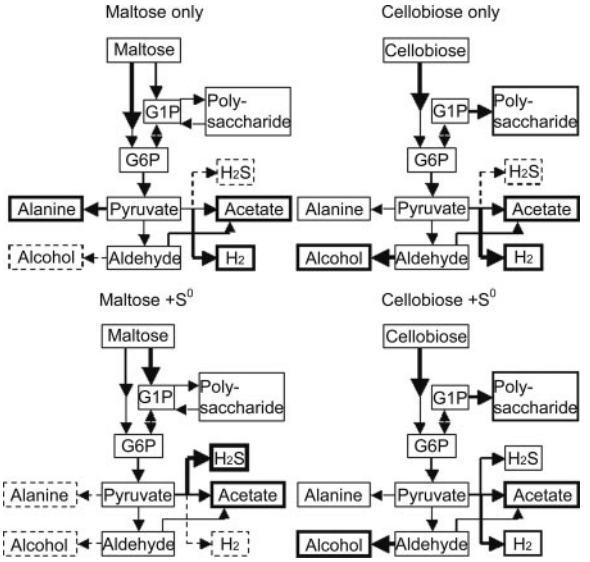

FIG. 3. Proposed metabolic pathways for *P. furiosus* grown on maltose and cellobiose in the presence and absence of S^0. The thickness of lines outlining boxes and of arrows reflects the significance of the product in the metabolic scheme. A dashed line indicates that the metabolite was not detected. G1P, glucose-1-phosphate; G6P, glucose-6-phosphate.

and H_2/CO_2 ratios and greater production of alanine instead of acetate, reduced ferredoxin, and subsequently H_2 (40). Thus, it appears that growth on maltose is somewhat limited because reducing power generated from substrate degradation was not involved in an H_2-producing, energy-conserving process (45). In contrast, growth on cellobiose triggered transcription of two alcohol dehydrogenases implicated in ethanol production from acetaldehyde, generated from pyruvate by POR (32). It has been proposed that this reaction removes the bottleneck in energy metabolism and detoxifies the cytoplasm by removing accumulating acetaldehyde, thereby facilitating pyruvate decarboxylation (33). Transcriptional analysis also suggested that capsular polysaccharide formation is increased in cellobiose-grown cultures, indicating another possible outlet for reducing equivalents during growth on this substrate. Alteration of metabolite profiles depending on carbon and energy sources has been noted in mesophilic fermentative bacteria (14). For example, inhibition of *Clostridium cellulolyticum* growth was relieved when cellobiose and yeast extract were replaced by cellulose and defined nitrogen sources (15). This effect was attributed to an imbalance in NADH/NAD ratios arising from higher carbon fluxes in addition to reduced demand on biosynthesis in the presence of complex substrates (22). Whether a similar situation exists for *P. furiosus* remains to be seen.

The addition of S^0 boosted biomass yields for both maltose- and cellobiose-grown cultures, albeit to a much greater extent for the maltose-grown cultures. This was reflected in the considerably higher number of differentially transcribed genes involved in anabolism and cellular redox management when S^0 was added to maltose. The close correlation between H_2S generation, biomass (protein) yield, and transcriptional levels of MBX and SipA/SipB suggests that S^0 reduction is an energy-conserving process in *P. furiosus* and not just a mechanism for

alleviating H_2 inhibition. While all H_2 production ceased in cultures grown on maltose plus S^0, with corresponding downregulation of MBH and SH1, only about one-third of the H_2 production was replaced by H_2S generation in cultures grown on cellobiose plus S^0. This very surprising result shows that in cellobiose-grown cultures regulation of the expression of MBH and MBX is not the on/off mechanism that appears to be present in maltose-grown cells, where the addition of S^0 causes hydrogen production and expression of the genes encoding the three hydrogenases to cease within minutes (Schut et al., unpublished data). At this point, it is not clear why *P. furiosus* metabolizes the two sugars so differently.

Both processes appear to use the same pathway from phosphorylated hexoses to the end products acetate, CO_2, and H_2 (plus H_2S) since the relative amounts of these compounds (per unit of sugar utilized) are the same (Table 2). However, not only do the H_2/H_2S ratios differ, but there is also a dramatic difference in carbon flow. For example, on cellobiose alone, about 75% of the sugar is converted to acetate and the gaseous products (sugar/acetate/H_2 ratio, ~1:1.5:3.8), whereas only 50% of the maltose is converted (sugar/acetate/H_2 ratio, 1:1:2.6). How the "extra" carbon from maltose is used is not known, but in bioenergy terms, if H_2 is the required product, then cellobiose should be the carbon source rather than maltose. Conversely, in the presence of S^0, the bioenergetics and end product yields and ratios are very similar (Table 2), indicating that the same pathways are utilized independent of the glycoside type. The one caveat is the production of H_2 by cellobiose-grown cells. In the presence of S^0, the metabolism of cellobiose in terms of end products (per unit of sugar) appears to be comparable to the metabolism of maltose (Table 2). Consequently, S^0 dramatically impacts the carbon flux from sugar into acetate in cellobiose-grown cells but has less impact in maltose-grown cells. Thus, S^0 affects carbon flux, in addition to its role as a reductant sink. At present, the transcriptional analyses do not provide insight into how S^0 achieves this in cellobiose-grown cells.

It is possible that the profound effect of the glycoside type on the S^0-dependent bioenergetics of *P. furiosus* extends to other hyperthermophiles, including bacteria. A homologous MBX operon can be identified in the genome of the facultative S^0-reducing hyperthermophilic bacterium *Thermotoga maritima*, probably as a result of lateral gene transfer (7). However, the transcriptional levels of this operon were relatively low on maltose and cellobiose and were not affected by S^0 (S. R. Gray and R. M. Kelly, unpublished data). A similar response was observed for two Sip homologs in *T. maritima*. It has been reported that S^0 stimulates *T. maritima* growth by removing inhibitory H_2 but does not impact energy conservation pathways (47).

An important outcome of this study is the realization that microbial processes aimed at high levels of H_2 production must take into account the impact that substrates and other environmental influences have on cellular bioenergetics. Given the anticipated heterogeneity of biomass feedstocks that will be used for bioenergy conversion processes, a comprehensive understanding of how transcriptional regulation and metabolite production relate to the substrate pool is highly desirable. By combining traditional approaches (chemostat culture for determining bioenergetic parameters) with functional genomics tools (transcriptional response analysis), insights can be obtained and ultimately provide the basis for metabolic engineering strategies. The information provided here for *P. furiosus* should prove to be useful in efforts to exploit H_2 production in this archaeon and other archaea for the production of biofuels.

ACKNOWLEDGMENTS

This work was supported in part by grants from the NASA Exobiology Program (grant EXB02-0000-0050 to R.M.K.), the DOE Energy Biosciences Program (grant DE-FG02-96ER20219 to R.M.K. and grant FG05-95ER20175 to M.W.W.A.), and the NSF Biotechnology Program (grants CBET-0317886 and CBET-0617272 to M.W.W.A. and R.M.K.). D.L.L. acknowledges support from a Department of Education GAANN Fellowship.

REFERENCES

1. **Adams, M. W.** 1993. Enzymes and proteins from organisms that grow near and above 100°C. Annu. Rev. Microbiol. **47:**627–658.
2. **Adams, M. W., J. F. Holden, A. L. Menon, G. J. Schut, A. M. Grunden, C. Hou, A. M. Hutchins, F. E. Jenney, Jr., C. Kim, K. Ma, G. Pan, R. Roy, R. Sapra, S. V. Story, and M. F. Verhagen.** 2001. Key role for sulfur in peptide metabolism and in regulation of three hydrogenases in the hyperthermophilic archaeon *Pyrococcus furiosus*. J. Bacteriol. **183:**716–724.
3. **Akutsu, J., Z. Zhang, M. Tsujimura, M. Sasaki, M. Yohda, and Y. Kawarabayasi.** 2005. Characterization of a thermostable enzyme with phosphomannomutase/phosphoglucomutase activities from the hyperthermophilic archaeon *Pyrococcus horikoshii* OT3. J. Biochem. **138:**159–166.
4. **Bauer, M. W., E. J. Bylina, R. V. Swanson, and R. M. Kelly.** 1996. Comparison of a beta-glucosidase and a beta-mannosidase from the hyperthermophilic archaeon *Pyrococcus furiosus*. Purification, characterization, gene cloning, and sequence analysis. J. Biol. Chem. **271:**23749–23755.
5. **Bevers, L. E., E. Bol, P. L. Hagedoorn, and W. R. Hagen.** 2005. WOR5, a novel tungsten-containing aldehyde oxidoreductase from *Pyrococcus furiosus* with a broad substrate specificity. J. Bacteriol. **187:**7056–7061.
6. **Blumentals, I. I., M. Itoh, G. J. Olson, and R. M. Kelly.** 1990. Role of polysulfides in reduction of elemental sulfur by the hyperthermophilic archaebacterium *Pyrococcus furiosus*. Appl. Environ. Microbiol. **56:**1255–1262.
7. **Calteau, A., M. Gouy, and G. Perriere.** 2005. Horizontal transfer of two operons coding for hydrogenases between bacteria and archaea. J. Mol. Evol. **60:**557–565.
8. **Chin, H. L., Z. S. Chen, and C. P. Chou.** 2003. Fedbatch operation using *Clostridium acetobutylicum* suspension culture as biocatalyst for enhancing hydrogen production. Biotechnol. Prog. **19:**383–388.
9. **Claassen, P. A. M., J. B. van Lier, A. M. L. Contreras, E. W. J. van Niel, L. Sijtsma, A. J. M. Stams, S. S. de Vries, and R. A. Weusthuis.** 1999. Utilisation of biomass for the supply of energy carriers. Appl. Microbiol. Biotechnol. **52:**741–755.
10. **Conners, S. B., C. I. Montero, D. A. Comfort, K. R. Shockley, M. R. Johnson, S. R. Chhabra, and R. M. Kelly.** 2005. An expression-driven approach to the prediction of carbohydrate transport and utilization regulons in the hyperthermophilic bacterium *Thermotoga maritima*. J. Bacteriol. **187:**7267–7282.
11. **Converti, A., and P. Perego.** 2002. Use of carbon and energy balances in the study of the anaerobic metabolism of *Enterobacter aerogenes* at variable starting glucose concentrations. Appl. Microbiol. Biotechnol. **59:**303–309.
12. **Costantino, H. R., S. H. Brown, and R. M. Kelly.** 1990. Purification and characterization of an alpha-glucosidase from a hyperthermophilic archaebacterium, *Pyrococcus furiosus*, exhibiting a temperature optimum of 105 to 115°C. J. Bacteriol. **172:**3654–3660.
13. **Cui, X., M. K. Kerr, and G. A. Churchill.** 2003. Transformations for cDNA microarray data. Stat. Appl. Genet. Mol. Biol **2:**Article 4.
14. **Desvaux, M.** 2006. Unravelling carbon metabolism in anaerobic cellulolytic bacteria. Biotechnol. Prog. **22:**1229–1238.
15. **Desvaux, M., E. Guedon, and H. Petitdemange.** 2001. Carbon flux distribution and kinetics of cellulose fermentation in steady-state continuous cultures of *Clostridium cellulolyticum* on a chemically defined medium. J. Bacteriol. **183:**119–130.
16. **Desvaux, M., E. Guedon, and H. Petitdemange.** 2001. Metabolic flux in cellulose batch and cellulose-fed continuous cultures of *Clostridium cellulolyticum* in response to acidic environment. Microbiology **147:**1461–1471.
17. **de Vos, W. M., S. W. Kengen, W. G. Voorhorst, and J. van der Oost.** 1998. Sugar utilization and its control in hyperthermophiles. Extremophiles **2:**201–205.
18. **Fiala, G., and K. O. Stetter.** 1986. *Pyrococcus furiosus* sp. nov. represents a novel genus of marine heterotrophic archaebacteria growing optimally at 100°C. Arch. Microbiol. **145:**56–61.
19. **Gao, J., M. W. Bauer, K. R. Shockley, M. A. Pysz, and R. M. Kelly.** 2003.

Growth of hyperthermophilic archaeon *Pyrococcus furiosus* on chitin involves two family 18 chitinases. Appl. Environ. Microbiol. **69:**3119–3128.
20. **Gray, K. A., L. Zhao, and M. Emptage.** 2006. Bioethanol. Curr. Opin. Chem. Biol. **10:**141–146.
21. **Gruyer, S., E. Legin, C. Bliard, S. Ball, and F. Duchiron.** 2002. The endopolysaccharide metabolism of the hyperthermophilic archeon *Thermococcus hydrothermalis*: polymer structure and biosynthesis. Curr. Microbiol. **44:**206–211.
22. **Guedon, E., M. Desvaux, S. Payot, and H. Petitdemange.** 1999. Growth inhibition of *Clostridium cellulolyticum* by an inefficiently regulated carbon flow. Microbiology **145:**1831–1838.
23. **Hallenbeck, P. C.** 2005. Fundamentals of the fermentative production of hydrogen. Water Sci. Technol **52:**21–29.
24. **Kadar, Z., T. de Vrije, G. E. van Noorden, M. A. Budde, Z. Szengyel, K. Reczey, and P. A. Claassen.** 2004. Yields from glucose, xylose, and paper sludge hydrolysate during hydrogen production by the extreme thermophile *Caldicellulosiruptor saccharolyticus*. Appl. Biochem. Biotechnol. **113-116:** 497–508.
25. **Kanai, T., H. Imanaka, A. Nakajima, K. Uwamori, Y. Omori, T. Fukui, H. Atomi, and T. Imanaka.** 2005. Continuous hydrogen production by the hyperthermophilic archaeon, Thermococcus kodakaraensis KOD1. J. Biotechnol. **116:**271–282.
26. **Kengen, S. W., J. E. Tuininga, F. A. de Bok, A. J. Stams, and W. M. de Vos.** 1995. Purification and characterization of a novel ADP-dependent glucokinase from the hyperthermophilic archaeon *Pyrococcus furiosus*. J. Biol. Chem. **270:**30453–30457.
27. **Kletzin, A., S. Mukund, T. L. Kelley-Crouse, M. K. Chan, D. C. Rees, and M. W. Adams.** 1995. Molecular characterization of the genes encoding the tungsten-containing aldehyde ferredoxin oxidoreductase from *Pyrococcus furiosus* and formaldehyde ferredoxin oxidoreductase from *Thermococcus litoralis*. J. Bacteriol. **177:**4817–4819.
28. **Kumar, N., and D. Das.** 2001. Continuous hydrogen production by immobilized *Enterobacter cloacae* IIT-BT 08 using lignocellulosic materials as solid matrices. Enzyme Microb. Technol. **29:**280–287.
29. **Lee, H. S., K. R. Shockley, G. J. Schut, S. B. Conners, C. I. Montero, M. R. Johnson, C. J. Chou, S. L. Bridger, N. Wigner, S. D. Brehm, F. E. Jenney, Jr., D. A. Comfort, R. M. Kelly, and M. W. Adams.** 2006. Transcriptional and biochemical analysis of starch metabolism in the hyperthermophilic archaeon *Pyrococcus furiosus*. J. Bacteriol. **188:**2115–2125.
30. **Lee, S. J., C. Moulakakis, S. M. Koning, W. Hausner, M. Thomm, and W. Boos.** 2005. TrmB, a sugar sensing regulator of ABC transporter genes in *Pyrococcus furiosus* exhibits dual promoter specificity and is controlled by different inducers. Mol. Microbiol. **57:**1797–1807.
31. **Ma, K., and M. W. Adams.** 1999. An unusual oxygen-sensitive, iron- and zinc-containing alcohol dehydrogenase from the hyperthermophilic archaeon *Pyrococcus furiosus*. J. Bacteriol. **181:**1163–1170.
32. **Ma, K., A. Hutchins, S. J. Sung, and M. W. Adams.** 1997. Pyruvate ferredoxin oxidoreductase from the hyperthermophilic archaeon, *Pyrococcus furiosus*, functions as a CoA-dependent pyruvate decarboxylase. Proc. Natl. Aca. Sci. USA **94:**9608–9613.
33. **Ma, K., H. Loessner, J. Heider, M. K. Johnson, and M. W. Adams.** 1995. Effects of elemental sulfur on the metabolism of the deep-sea hyperthermophilic archaeon *Thermococcus* strain ES-1: characterization of a sulfur-regulated, non-heme iron alcohol dehydrogenase. J. Bacteriol. **177:**4748–4756.
34. **Ma, K., R. N. Schicho, R. M. Kelly, and M. W. Adams.** 1993. Hydrogenase of the hyperthermophile *Pyrococcus furiosus* is an elemental sulfur reductase or sulfhydrogenase: evidence for a sulfur-reducing hydrogenase ancestor. Proc. Natl. Acad. Sci. USA **90:**5341–5344.
35. **Ma, K., R. Weiss, and M. W. Adams.** 2000. Characterization of hydrogenase II from the hyperthermophilic archaeon *Pyrococcus furiosus* and assessment of its role in sulfur reduction. J. Bacteriol. **182:**1864–1871.
36. **Musfeldt, M., M. Selig, and P. Schonheit.** 1999. Acetyl coenzyme A synthetase (ADP forming) from the hyperthermophilic archaeon *Pyrococcus furiosus*: identification, cloning, separate expression of the encoding genes, *acdAI* and *acdBI*, in *Escherichia coli*, and in vitro reconstitution of the active heterotetrameric enzyme from its recombinant subunits. J. Bacteriol. **181:** 5885–5888.
37. **Nath, K., and D. Das.** 2004. Improvement of fermentative hydrogen production: various approaches. Appl. Microbiol. Biotechnol. **65:**520–529.
38. **Ogino, H., T. Miura, K. Ishimi, M. Seki, and H. Yoshida.** 2005. Hydrogen production from glucose by anaerobes. Biotechnol. Prog. **21:**1786–1788.
39. **Pysz, M. A., S. B. Conners, C. I. Montero, K. R. Shockley, M. R. Johnson, D. E. Ward, and R. M. Kelly.** 2004. Transcriptional analysis of biofilm formation processes in the anaerobic, hyperthermophilic bacterium *Thermotoga maritima*. Appl. Environ. Microbiol. **70:**6098–6112.
40. **Rinker, K. D., and R. M. Kelly.** 2000. Effect of carbon and nitrogen sources on growth dynamics and exopolysaccharide production for the hyperthermophilic archaeon *Thermococcus litoralis* and bacterium *Thermotoga maritima*. Biotechnol. Bioeng **69:**537–547.
41. **Rinker, K. D., and R. M. Kelly.** 1996. Growth physiology of the hyperthermophilic archaeon *Thermococcus litoralis*: development of a sulfur-free defined medium, characterization of an exopolysaccharide, and evidence of biofilm formation. Appl. Environ. Microbiol. **62:**4478–4485.
42. **Roy, R., and M. W. Adams.** 2002. Characterization of a fourth tungsten-containing enzyme from the hyperthermophilic archaeon *Pyrococcus furiosus*. J. Bacteriol. **184:**6952–6956.
43. **Rupprecht, J., B. Hankamer, J. H. Mussgnug, G. Ananyev, C. Dismukes, and O. Kruse.** 2006. Perspectives and advances of biological H_2 production in microorganisms. Appl. Microbiol. Biotechnol. **72:**442–449.
44. **Sakuraba, H., S. Goda, and T. Ohshima.** 2004. Unique sugar metabolism and novel enzymes of hyperthermophilic archaea. Chem. Rec. **3:**281–287.
45. **Sapra, R., K. Bagramyan, and M. W. Adams.** 2003. A simple energy-conserving system: proton reduction coupled to proton translocation. Proc. Natl. Acad. Sci. USA **100:**7545–7550.
46. **Schicho, R. N., K. Ma, M. W. Adams, and R. M. Kelly.** 1993. Bioenergetics of sulfur reduction in the hyperthermophilic archaeon *Pyrococcus furiosus*. J. Bacteriol. **175:**1823–1830.
47. **Schroder, C., M. Selig, and P. Schonheit.** 1994. Glucose fermentation to acetate, CO_2 and H_2 in the anaerobic hyperthermophilic eubacterium *Thermotoga maritima*—involvement of the Embden-Meyerhof pathway. Arch. Microbiol. **161:**460–470.
48. **Schut, G. J., S. D. Brehm, S. Datta, and M. W. Adams.** 2003. Whole-genome DNA microarray analysis of a hyperthermophile and an archaeon: *Pyrococcus furiosus* grown on carbohydrates or peptides. J. Bacteriol. **185:**3935–3947.
49. **Schut, G. J., J. Zhou, and M. W. Adams.** 2001. DNA microarray analysis of the hyperthermophilic archaeon *Pyrococcus furiosus*: evidence for an new type of sulfur-reducing enzyme complex. J. Bacteriol. **183:**7027–7036.
50. **Shockley, K. R.** 2004. Functional genomics investigation of microbial physiology in the hyperthermophilic microorganism *Pyrococcus furiosus* and *Thermotoga maritima.* Ph. D. thesis. North Carolina State University, Raleigh.
51. **Shockley, K. R., D. E. Ward, S. R. Chhabra, S. B. Conners, C. I. Montero, and R. M. Kelly.** 2003. Heat shock response by the hyperthermophilic archaeon *Pyrococcus furiosus*. Appl. Environ. Microbiol. **69:**2365–2371.
52. **Silva, P. J., E. C. van den Ban, H. Wassink, H. Haaker, B. de Castro, F. T. Robb, and W. R. Hagen.** 2000. Enzymes of hydrogen metabolism in *Pyrococcus furiosus*. Eur. J. Biochem. **267:**6541–6551.
53. **Tachdjian, S., and R. M. Kelly.** 2006. Dynamic metabolic adjustments and genome plasticity are implicated in the heat shock response of the extremely thermoacidophilic archaeon *Sulfolobus solfataricus*. J. Bacteriol. **188:**4553–4559.
54. **van der Oost, J., W. G. Voorhorst, S. W. Kengen, A. C. Geerling, V. Wittenhorst, Y. Gueguen, and W. M. de Vos.** 2001. Genetic and biochemical characterization of a short-chain alcohol dehydrogenase from the hyperthermophilic archaeon *Pyrococcus furiosus*. Eur. J. Biochem. **268:**3062–3068.
55. **van Haaster, D. J., P. L. Hagedoorn, J. A. Jongejan, and W. R. Hagen.** 2005. On the relationship between affinity for molecular hydrogen and the physiological directionality of hydrogenases. Biochem. Soc. Trans. **33:**12–14.
56. **van Lieshout, J., M. Faijes, J. Nieto, J. van der Oost, and A. Planas.** 2004. Hydrolase and glycosynthase activity of endo-1,3-beta-glucanase from the thermophile *Pyrococcus furiosus*. Archaea **1:**285–292.
57. **van Niel, E. W., P. A. Claassen, and A. J. Stams.** 2003. Substrate and product inhibition of hydrogen production by the extreme thermophile, *Caldicellulosiruptor saccharolyticus*. Biotechnol. Bioeng **81:**255–262.
58. **Van Ooteghem, S. A., S. K. Beer, and P. C. Yue.** 2002. Hydrogen production by the thermophilic bacterium *Thermotoga neapolitana*. Appl. Biochem. Biotechnol. **98-100:**177–189.
59. **Voorhorst, W. G., R. I. Eggen, E. J. Luesink, and W. M. de Vos.** 1995. Characterization of the *celB* gene coding for beta-glucosidase from the hyperthermophilic archaeon *Pyrococcus furiosus* and its expression and site-directed mutation in *Escherichia coli*. J. Bacteriol. **177:**7105–7111.
60. **Ward, D. E., S. W. Kengen, J. van Der Oost, and W. M. de Vos.** 2000. Purification and characterization of the alanine aminotransferase from the hyperthermophilic archaeon *Pyrococcus furiosus* and its role in alanine production. J. Bacteriol. **182:**2559–2566.
61. **Williams, E., T. M. Lowe, J. Savas, and J. Diruggiero.** 2007. Microarray analysis of the hyperthermophilic archaeon *Pyrococcus furiosus* exposed to gamma irradiation. Extremophiles **11:**19–29.
62. **Xavier, K. B., R. Peist, M. Kossmann, W. Boos, and H. Santos.** 1999. Maltose metabolism in the hyperthermophilic archaeon *Thermococcus litoralis*: purification and characterization of key enzymes. J. Bacteriol. **181:**3358–3367.